Effect of Formation Conditions on the Structure and Properties of Nanocomposite Alginate Fibers

Maciej Boguń,[1] Teresa Mikołajczyk,[1] Stanisław Rabiej[2]

[1]*Department of Man-Made Fibres, Faculty of Material Technologies and Textile Design, Technical University of Lodz, Poland*
[2]*Institute of Textile Engineering and Polymer Materials, Faculty of Materials and Environment Sciences, University of Bielsko, Biała*

Received 6 January 2009; accepted 8 March 2009
DOI 10.1002/app.30465
Published online 28 May 2009 in Wiley InterScience (www.interscience.wiley.com).

ABSTRACT: The conditions for producing nanocomposite fibers composed of calcium alginate, containing a hydroxyapatite nanoadditive were devised and the rheological, sorptive, and strength properties of these fibers, as well as their porous and supramolecular structure were subjected to analysis. It has been concluded that the presence of the HAp nanoadditive in the material of alginate fibers decreases their susceptibility to distortion in the drawing stage, which results in their tenacity properties being lower by 2cN/tex than of the fibers with no nanoadditive. The obtained nanocomposite fibers are characterised by a tenacity value exceeding 26 cN/tex, accompanied by high sorptive and water-retention properties of 90% and the even distribution of the nanoadditive on the fiber surface. © 2009 Wiley Periodicals, Inc. J Appl Polym Sci 114: 70–82, 2009

Key words: biopolymers; fibers; nanocomposites; WAXS

INTRODUCTION

The occurrence of complex bone fractures and degenerative bone diseases is the reason for searching for new biomaterials that would support and stimulate the process of bone regeneration.

Currently, the biomaterials based on natural polymers such as cellulose, chitin, and sodium alginate are gaining recognition in the fields of material engineering. All of these polymers are broadly used in the production of specialist dressings. Tissue engineering may be a new area of application for them.

One of the polymers most widely used in medicine is the alginate.[1] It is a linear polysaccharide composed of the residues of the β-D-mannuronic acid (M) and the α-L-guluronic acid (G),[2] which usually reveals an alternating structure of the type MMMGGGMG.[3] From the point of view of medical application, this polymer is characterised by very important properties, such as, the lack of toxicity, antibacterial properties, a unique tissue compatibility, and controlled biodegradation. Various forms of alginates are being used in tissue engineering for the treatment and regeneration of skin, cartilage, liver, and the myocardial tissue.[4–8]

Correspondence to: M. Boguń (maciek.bogun@wp.pl).
Contract grant sponsor: Research financed by the Minister of Science and Higher Education in 2007-2010 as development project No. 0564/R/T02/2007/03.

A peculiar group of biomaterials is represented by alginate fibers–specifically calcium alginate fibers obtained through substituting Na^+ ions with Ca^{++} ions in a solidifying bath. These fibers have found wide application in the manufacturing of modern dressings, bandages, and absorbents, which react with the wound mucus and become partly gelled, facilitating the dressing change and decreasing the patient's pain.

Many scientific institutions are currently exploring an innovative area of research, namely, the application of nanotechnology in tissue engineering. Available publications on the topic include many studies on the use of biopolymers in the production of nanofibers used for manufacturing 3D-scaffolds and various types of membranes.[9,10] An alternative solution to such biomaterials may be the nanocomposite alginate fibers, obtained through the traditional spinning method, and used in the production of various types of biocomposites. For example, introducing ceramic nanoadditives into the fibers would result in obtaining biocomposites with unprecedented biological properties. The ceramic material which is revolutionising modern medicine is hydroxyapatite or calcium orthophosphate ($Ca_{10}(PO_4)_6(OH)_2$) with a molar Ca/P ratio of 1.667 and containing hydroxyls.[11] Its significance for modern medicine stems from the fact that it is one of the most biocompatible chemical compounds, constituting about 69% of total bone mass.[12–16] Hydroxyapatite has its application in dentistry, maxillary and facial surgery, orthopaedics, as a drug carrier, and an ingredient of cell culture

beds.[17,18] It can also be used as a nanoadditive for polymer dyes in the production of scaffolds for tissue engineering.[19,20]

The purpose of the present study was to determine the influence of the as-spun draw ratio and the related deformation value in the drawing stage on the strength properties, porous structure, and sorptive properties of calcium alginate fibers containing HAp additive. The results will enable the identification of the production conditions for nanocomposite alginate fibers with a tenacity exceeding 20cN/tex and enhanced sorption. The fibers will make up a biocomposite prepared based on another resorbable polymer (polylacitide or ε-caprolactone) used in the treatment of bone defects.

The influence of the presence of hydroxyapatite in the material of the fibers is determined based on a comparative analysis of the structural parameters and properties of nanocomposite fibers with respective parameters of fibers without the nanoadditive.

EXPERIMENTAL

Materials

In the preparation of yarn solutions, we used sodium alginate manufactured by FMC Biopolimer (Norway), trade name Protanal LF 10/60LS, with specific viscosity $\eta = 3.16$ dL/g.

This polymer is characterised by the predominance of blocks originating from mannuronic acid (up to 65%) in relation to residues of the guluronic acid. The nanoadditive used was natural hydroxyapatite synthesised at AGH Kraków (University of Science and Technology in Cracow) according to the patent.[21] The characterization of the nanoadditive was performed at AGH Kraków, and it included the measuring of its surface extension with the BET method (gas adsorption), determining the size of particles by means of (DLS), and the microscopic observation of these particles (SEM).

The measurement of the specific surface was conducted by means of the NOVA 1200e analyser (Quantachrome Inst.), using the BET adsorption isotherm method.

The size of particles was measured with the use of the Zetasizer Nano-ZS (Malvern, Instruments Limited, UK) by means of the Dynamic Light Scattering technique.

The applied hydroxyapatite is characterised by an average specific surface in the order of 73.6 m^2/g, and the size of particles ranges from 30 to 500 nm.

Fiber formation

The alginate fibers were formed with the wet-spinning from solution method using distilled water as the solvent. Based on the preliminary examinations, the concentration of sodium alginate in water at the level of 7.4% and the nanoadditive content of 3% in proportion to the polymer mass were selected.

Before being added to the spinning solution, the nanoadditive suspension was subjected to a 30 min ultrasound treatment. For this purpose, the 100-Watt Sonopuls sounder (Bandelin) was used.

The fibers were manufactured in a commercial-lab spinner whose structure enabled the stabilising of technological parameters on desired levels, as well as their constant supervision and broad-range of possibilities in changing the process parameters. The solidification of calcium alginate fibers was conducted in a bath containing $CaCl_2$ and HCl. The drawing process consisted of two stages: The first stage of drawing took place in a plastification bath containing $CaCl_2$ and a small quantity of 0.03% solution of HCl. The second stage took place in saturated water vapour at a temperature of 135°C. The fibers were drawn in a continuous manner, by winding them on a reel. Following the drawing and rinsing, the fibers were dried in isometric conditions at a temperature of 25°C.

Research methods

The rheological properties of spinning solutions were determined using an Anton Paar rotational rheometer. The measurement was conducted with regard to the shearing speed of 145 1/s at the temperature of 20°C with the use of an H-type cylinder. Rheological parameters n and K were determined on the basis of flow curves presented in a logarithmic arrangement.

The tenacity of the fibers was determined in compliance with the PN-EN ISO 5079 : 1999 standard.

Water vapour sorption was established in the conditions of 65% and 100% relative humidity in compliance with the Polish Standard PN-71/P-04653.

Water retention was determined with the use of a laboratory centrifuge, which enabled a mechanical disposal of water from the fibers in the centrifugation process with the acceleration of 10,000 m/s^2. The retention value was designated as the ratio of water mass remaining in the fiber after centrifugation to the mass of the totally dried fiber.

The porosity of the fibers was measured by means of mercury porosimetry, using the Carlo-Erba porosimeter coupled with a computer, enabling the estimation of the total volume of the pores, the percentage of pores ranging between 5 and 7500 nm in size, as well as the total internal surface of the pores.

The distribution of the HAp nanoadditive in the fiber was assessed on the basis of photographs made with the use of scanning electron microscopy (SEM JSM 5400) equipped with an *EDX LINK ISIS* energy dispersion analyser for specific radiation (Oxford Instruments).

Degree of crystallinity and size of crystallites were determined using wide angle X-ray diffraction (WAXS) method. Diffraction patterns were recorded in a symmetrical reflection mode using URD 6 Seifert diffractometer and a copper target X-ray tube (λ = 0.154 nm) operated at 40 kV and 30 mA. Cu Kα radiation was monochromized with a crystal monochromator. WAXS curves were recorded in the range $2^o - 60^o$, with a step of 0.1^o and the registration time of 30 s per step Investigated fibers were powdered and pressed into a sample holder. Samples with the radius of 2 cm and the thickness of 1 mm were prepared.

The diffraction curves of alginate fibers were analyzed by means of a computer program WAXSFIT.[22,23] In the first stage, a linear background was determined based on the intensity level at small and large angles and subtracted from the diffraction curve. Moreover, the curves of all samples were normalized to the same value of integral intensity scattered by a sample over the whole range of scattering angle recorded in the experiment. Next, the diffraction curves were resolved into crystalline peaks and amorphous component. To this aim, a theoretical curve was constructed, composed of functions related to individual crystalline peaks and amorphous halos. The theoretical curve was fitted to the experimental one using a multicriterial optimization procedure and a hybrid system which combines a genetic algorithm and a classical optimization method of Powell.[24] Both crystalline peaks and amorphous halos, were represented by linear combination of Gauss and Lorentz profiles. The amorphous component was approximated by two broad maxima located at $2\theta \approx 21^o$, and $2\theta \approx 40^o$.

Degree of crystallinity was calculated as the ratio of the total, integral intensity comprised in the crystalline peaks to the total, integral intensity scattered by a sample over the whole range of measurement, after the background subtraction.

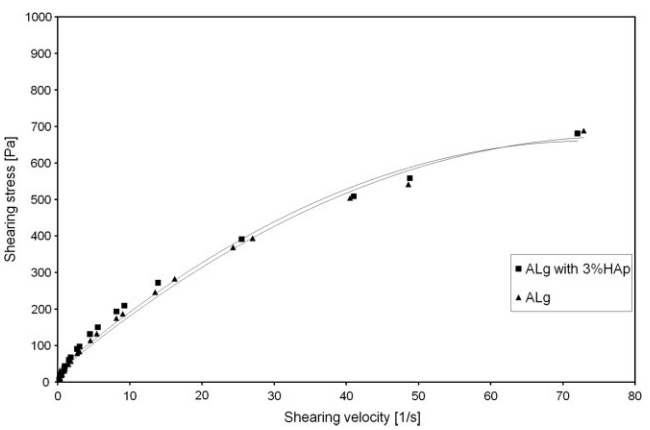

Figure 1 The relationship between shearing stress and the shearing velocity for 7.4% sodium alginate solutions LF 10/60/LS with and without the HAp nanoadditive.

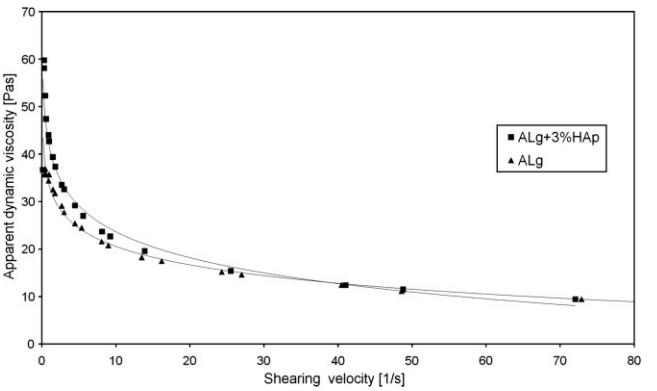

Figure 2 The relationship between apparent dynamic viscosity in the shearing velocity function for 7.4% sodium alginate solutions LF 10/60/LS with and without the HAp nanoadditive.

RESULTS AND DISCUSSION

Rheological properties of spinning solutions

It is a well-known fact that the rheological properties of a liquid determine the distribution of its flow velocity in the filiera channel, the scale of the stream expansion effect, and the variations in the longitudinal velocity gradient along the formation route, related to the reception force. The rheological qualities of a liquid also influence the stress values in the solidification stage.

Based on the analysis of obtained flow curves (Fig.1) of the spinning solution both with and without the nanoadditive, it may be concluded that both of these substances are non-Newtonian liquids, shearing-diluted, and with no flow limit. In both cases, the tangential stress increased less than proportionately to the increase in shearing velocity, and the curves pass through the coordinate origin. Apparent dynamic viscosity, however, decreases with the coagulation rate, a feature typical of polymer liquids. Increased proportion of the nano-additive does not change the nature of this relationship (Fig.2).

The introduction of the nanoadditive did not alter the rheological character of the liquid; however, it did influence the value of the n and k rheological parameters (Table I).

The presence of the nano-additive in the solution led to the increasingly non-Newtonian nature of the liquid and increased rheological parameter k. The parameter is a measure of consistence of the

TABLE I
The Rheological Properties of the Spinning Solution

Sample symbol	Rheological parameter n	Rheological parameter k
7.4% Alg Na^+	0.719	36.35
7.4% Alg Na^+ + 3% HAp	0.637	43.78

TABLE II
Calcium Alginate Fiber Formation Variants

			First drawing process		Second drawing process
	Solidification baths		Plastification baths		Saturated water vapour
Sample symbol	Temperature [°C]	Content of $CaCl_2$ [%]	Temperature [°C]	Content of $CaCl_2$ [%]	Temperature [°C]
AP 1	20	3	70	3	135
AP 2	40	3	70	3	135
AP 3	20	5	70	7	135
AP 4	40	5	70	7	135

solution. Such influence of the nanoadditive presence on the rheological behaviour of the liquid may be explained in the following way:

According to the well-known explanation of the mechanism of dilution by shearing in a static liquid,[25] there is a significant entanglement of macromolecules with the continuous phase (solvent) trapped between them. Introducing the relatively large HAp nanoadditive into this system leads to the effective enlargement of such clusters. During coagulation, macromolecules straighten and unwind with the increasing coagulation rate. In consequence, the internal friction of the system goes down due to the disintegration of clusters. Simultaneously, the presence of nano-hydroxyapatite facilitates gradual stripping of the solvation envelope with the increased coagulation rate. This also leads to the decreased internal friction of the system. This is related to the rise of the rheological k parameter, since this effect requires a greater value of stress.

Selection of the temperature and concentration of the solidifying bath in the process of fiber formation

Obviously, the calcium chloride content in the solidifying bath is the basic parameter determining the extent of the substitution of sodium ions with calcium ions in the calcium alginate of which the fibers are built. The speed of this process may also be influenced by the temperature of the solidifying bath. To determine the temperature and $CaCl_2$ concentration in the solidifying and plastification baths, four different options of calcium alginate fiber formation were tested. The consecutive stages of the formation process for all the variants, together with their characteristic parameters, are shown in Table II.

Fiber formation conditions were selected on the basis of the following criteria:

- The maximum calcium content in the fiber, and
- The best possible strength properties of the fibers.

Characteristic features of the fibers formed in particular variants are presented in Table III.

Research analysis reveals that the highest values of strength can be obtained by applying an increased $CaCl_2$ concentration both in the solidifying bath, and in the plastification bath. As far as the calcium content is concerned, it tends to be the highest in fibers formed in a 3% $CaCl_2$ bath at a temperature of 40°C (104°F). What is more, such fibers still preserve a relatively high tenacity (exceeding 23 cN/tex). Taking into account the application of the fibers in implants whose aim is to support and stimulate the process of bone regeneration, a high calcium content is very desirable. The lower content of calcium in fibers solidified and subjected to the stretching process in baths with a higher $CaCl_2$ content may be caused by the excessive "precipitation force," and, therefore, formation of a rigid film of solidified polymer at the phase boundary. Its presence hinders the substitution of sodium ions in sodium alginate with calcium ions from the coagulation bath. This phenomenon may become even more intensive upon the

TABLE III
Properties of Calcium Alginate Fibers Formed at Different Concentrations of the Solidifying and Plastification Baths

Sample symbol	As-spun draw ratio [%]	Total drawing [%]	Total deformation	Tenacity [cN/tex]	Elongation at break [%]	Content of Ca^{++} [%]
AP 1	70	63.10	3.0988	20.63 ± 0.78	8.38 ± 0.25	8.15 ± 0.24
AP 2	70	93.83	3.6827	23.48 ± 0.87	9.45 ± 0.47	9.22 ± 0.28
AP 3	70	96.63	3.7360	26.71 ± 0.14	8.58 ± 0.51	8.59 ± 0.26
AP 4	70	81.34	3.4454	25.70 ± 0.94	9.07 ± 0.36	7.66 ± 0.23

introduction of nanoadditives to the spinning solution, hampering the substitution processes. We observed a similar influence of nanoadditives in the case of another fiber-forming material.[26] Therefore, the best option seems to be to conduct the fiber formation process in a solidifying bath containing 3% of $CaCl_2$ at a temperature of 40°C. The drawing process should be conducted at the first stage in a bath with the same proportion of calcium chloride. Fibers obtained in this manner are characterised by a high calcium content of 9.22% (with the maximum theoretical proportion estimated based on the chemical reaction being 10.27%) and tenacity value exceeding 23 cN/tex.

Analysis of the porous structure and sorptive properties of alginate fibers

Employing the formation conditions described above, research was conducted with regard to the influence of the as-spun draw ratio and related value of total draw ratio on the porous structure, as well as sorptive and strength properties of calcium alginate fibers with and without a hydroxyapatite nanoadditive dispersed in the material. Research results are shown in Table IV.

As we know, the final properties of the fibers depend on the structure created at the solidification stage and its susceptibility to distortion at the drawing stage. It may be assumed that, with a rigid macromolecular structure of the material, one significant feature is the deformation of the still liquid stream, dependent on the as-spun draw ratio. Applying positive values of this ratio is conducive to the orientation of structural elements in the gradually solidifying stream, which is related to the strength properties of the fibers. The value of the as-spun draw ratio determines both the total volume of pores, and the nature of the generated porous structure.

In general, the porosity of fibers is a resultant of the formation conditions and the related factor of the solidification mechanism and the behaviour of the polymer solution at this stage of the process. In the case of fibers containing alginates of bivalent metals, it is assumed that the process of ion substitution is accompanied by the gelling stage. Such gels undergo syneresis during which their structure becomes condensed. The type of gel created depends on the structure of the fiber material. It is a fact, that in the case of high-guluronic acid alginates, so-called "hard gels" are produced, which are highly subjective to syneresis, which in turn leads to obtaining fibers with lower porosity.[27] When the molecular chain is dominated by blocks of mannuronic-acid origin, the gels are "soft." Obtaining fibers with a much higher porosity (Table IV) suggest that gels of this type are less susceptible to syneresis. As a result, the structure of the solidifying fiber becomes less condensed. It may also be seen in the cross section of the fibers, which is nearly circular in shape (Fig. 3).

By contrast, the fibers produced from high-guluronic acid alginate have displayed a flattened cross-section, resembling the shape of a bean seed.[27]

The analysis of the variations in the total volume of pores in the function of the as-spun draw ratio (Table IV) reveals that the highest value of this factor is characteristic for fibers formed at a +70% ratio in the case of calcium alginate fibers, and at a +90% ratio in the case of such fibers containing the dispersed HAp nanoadditive. In these fibers, the largest total volume of pores is concurrent with a high value of internal pore surface. This determines the nature of the structure and high proportions of small pores (4 to 12.3 nm), compared with other fibers.

It is manifested by the occurrence of the first maximum value on the graph illustrating the percentage of pores in the function of their radius (Fig. 4). For both types of fibers, the lowest value of total pore

TABLE IV
The Porous Structure and Sorptive Properties of Calcium Alginate Fibers with and Without Nanoadditive

Sample symbol	As-spun draw ratio [%]	Total drawing [%]	Content of Ca^{++} [%]	Total volume of pores [cm^3/g]	Total internal surface of pores [m^2/g]	Moisture sorption at 65% RH [%]	Moisture sorption at 100% RH [%]	Water retention [%]
AC 1	+50	101.78	8.66	0.102	10.51	24.63 ± 0.74	47.98 ± 1.44	101.46 ± 3.24
AC 2	+70	120.40	8.85	0.376	50.71	24.14 ± 0.72	47.59 ± 1.22	83.00 ± 2.25
AC 3	+90	109.18	9.00	0.203	14.00	24.49 ± 0.73	47.56 ± 0.98	86.23 ± 1.98
AC 4	+110	87.81	8.72	0.257	21.51	24.45 ± 0.98	47.25 ± 1.68	88.87 ± 2.45
AC 5	+120	97.00	9.13	0.303	31.13	24.41 ± 0.97	47.27 ± 1.01	84.98 ± 2.84
AH 1	+50	110.66	8.96	0.139	4.93	25.39 ± 1.02	48.23 ± 1.24	94.74 ± 3.01
AH 2	+70	103.58	9.46	0.222	11.90	24.21 ± 0.73	44.03 ± 0.99	90.15 ± 2.74
AH 3	+90	97.90	9.08	0.245	21.15	24.38 ± 0.97	44.57 ± 0.89	84.50 ± 1.99
AH 4	+110	99.72	9.80	0.220	4.67	24.07 ± 0.69	46.81 ± 0.75	83.86 ± 1.64
AH 5	+120	76.92	9.84	0.213	3.02	24.50 ± 0.99	46.44 ± 1.24	95.98 ± 2.24

AC – fibers without nanoadditive; AH – fibers with nanoadditive.

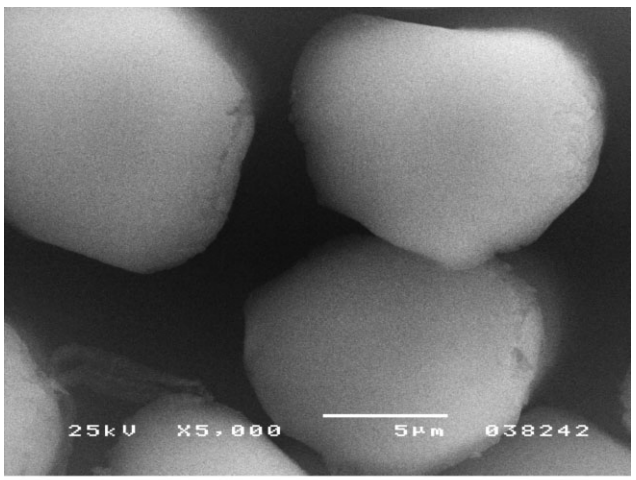

Figure 3 Cross section of the fibers: a) with HAp nanoadditive; b) without nanoadditive.

volume is displayed by fibers formed at the as-spun draw ratio of +50%. In all cases, except for sample AC 2, the nature of the porous structure may be classified as macroporous, as the total proportion of large and very large pores exceeds 50%.

As concluded from our previous research on the introduction of various nanoadditives to fibers made of different fiber-forming materials (e.g. polyacrylonitrile – PAN),[28] the presence of such intrusions entails an increase in fiber porosity. However, in the case of high-mannuronic acid calcium alginate fibers containing HAp, the total volume of pores is comparable or even slightly smaller in comparison to fibers without the nanoadditive. Despite of the differences in the total pore volume in both types of fibers in the function of the as-spun draw ratio, variations in humidity sorption both for 65% RH, and 100% RH are inconsiderable, ranging from 24.07% to 25.39%, and 44.03% to 48.23%, respectively. This fact suggests that sorptive properties of fibers are determined by the hydrophilic nature of the material. The process of moisture absorption by capillary condensation, related to moisture absorption at 100% RH, is less important. Meanwhile, the water retention value is mainly dependent on the nature of porous structure and the proportion of large and very large pores. In fibers made of hydrophobic materials, the latter ones are unable to retain water after it had been mechanically removed. However, in the case of calcium alginate fibers, it is possible for polymorphic water clusters to be bound to unsubstituted–OH groups of the material by means of hydrogen bridges.[29] This explains the fact that both types of fibers formed at the as-spun draw ratio of +50%, despite the lowest values of total pore volume and total internal pore surface, are characterised by the highest (or some of the highest, in the case of fibers with nanoadditive) water retention values. The lack of usual coincidence in the water retention change process and the total volume of pores in the function of as-spun draw ratio for both types of fibers is evidential to the important influence of the nature of the porous structure on the value of this ratio.

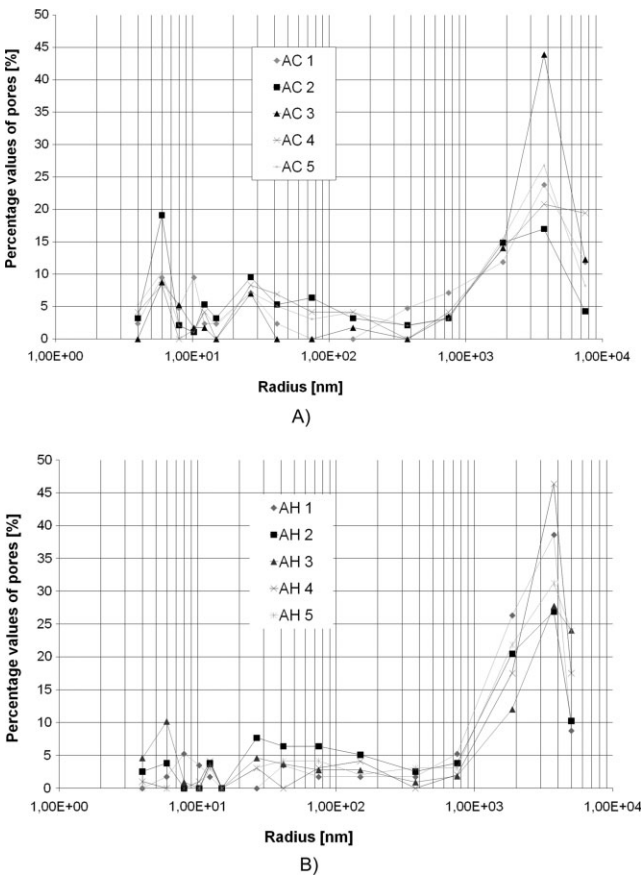

Figure 4 Relationship between the percentage values of pores in the function of their radius for: fibers without nanoadditive fibers with nanohydroxyapatite content.

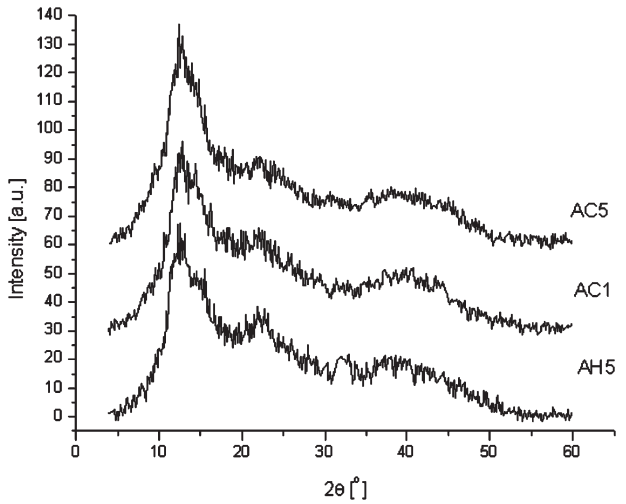

Figure 5 WAXS curves of alginate fibers after the background subtraction and normalization. AH1- fibers with the nanoadditive Hap formed with the as spun draw ratio of +120% AC1- fibers without the nanoadditive Hap formed with the as spun draw ratio of +50% AC5- fibers without the nanoadditive Hap formed with the as spun draw ratio of +120%.

Analysis of the crystalline structure of the fibers

Figure 5 shows the normalized WAXS curves of two types of alginate fibers without HAp, formed with the lowest (+50%) and the highest (+120%) as-spun draw ratio and of one fiber containing the nanoadditive, also formed with the highest (+120%) as-spun draw ratio. As one can see, all curves are very similar to one another. This fact suggests, that neither the forming conditions nor the presence of the nanoadditive, influence considerably the degree of crystallinity and the quality of the crystalline structure of fibers.

The curves are shifted in vertical direction for better visualization.

To calculate the degree of crystallinity, the diffraction curves were resolved into individual crystalline peaks. The resolution was performed considering a composed structure of the macromolecules of alginates. The blocks of α-L-guluronic acid residues (G blocks) and blocks of β-D-mannuronic acid residues (M blocks) form the crystalline structures of different parameters. For this reason, the shape of the WAXS curve of a given alginate sample depends on its chemical composition. In particular, it is dependent on the lengths and localization of the G and M blocks. According to Atkins et al.,[30] the unit cells of both polymannuronic acid and polyguluronic acid are orthorombic but their dimensions differ considerably. In the case polymannuronic acid, they are equal to: **a** = 0.76 nm, **b** = 0.86 nm and **c** = 1.04 nm (chain axis). For the polyguluronic acid, they amount to: **a** = 0.86 nm, **b** = 1.07 nm and **c** = 0.87. In both structures two antiparallel, twofold helical chains (2_1) pass through each unit cell. The basic element of both mannuronic acid and guluronic acid residues is the tetrahydropyranose ring and this has two different conformations. In the first case it assumes the $^4C_1$ conformation and in the second case the $^1C_4$ conformation. Because of different conformations of M and G mers, the shapes of macromolecules differ considerably. The macromolecule of polymannuronic acid is relatively straight like a flat ribbon, whereas the macromolecule of polyguluronic acid is buckled and adopts a characteristic zigzag shape. The schemes of both macromolecules are shown in Figure 6.

So, in the fibers produced of calcium alginate, two types of crystalline regions are present–the regions composed of M blocks and those ones of G blocks. This fact is seen in the shapes of the diffraction curves which show the cystalline peaks arising from both types of crystallites. From the unit cell dimensions listed above, the interplanar distances d_{hkl} for different families of lattice planes were calculated. Next, using Bragg's law, the 2θ angular positions of crystalline reflections related to the lattice planes were calculated. In this way, the Miller's indices of the crystalline peaks observed in the WAXS patterns

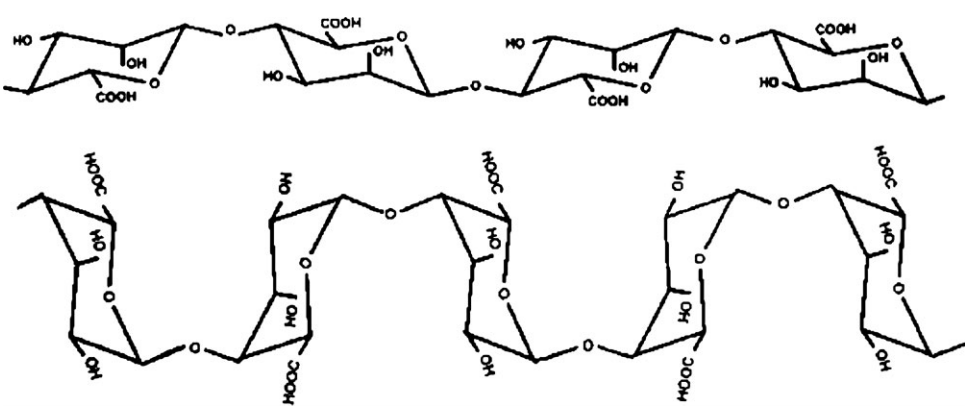

Figure 6 Schematic presentation of the macromolecules of polymannuronic (top) and polyguluronic acids (bottom).[31]

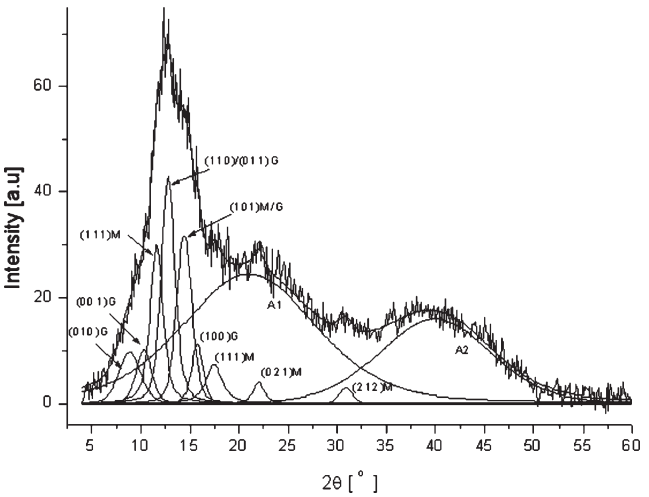

Figure 7 Diffraction curve of the alginate fiber formed with the as spun draw ratio of +120% (sample AC5) resolved into components. The Miller indices of crystalline peaks are shown in the figure. The peaks related to the crystallites composed of mannuronic and guluronic blocks are denoted by M and G letters, respectively. Amorphous components are denoted by A1 and A2 symbols.

were established. As an example, the diffraction curve of an alginate fiber resolved into crystalline peaks and amorphous components is shown in Figure 7.

In the performed analysis, the influence of calcium ions introduced into the fiber material has also been taken into consideration. According to the "egg-box" model proposed by Grant et al.,[32] part of Ca^{2+} ions is localized in the cavities that are formed between extended, parallel G blocks of two adjacent macromolecules. Such an embodiment of the calcium ions is possible because of the specific zigzag shape of the blocks (Fig. 8). As a result, two parallel G blocks are connected with one another not only by the hydrogen bonds but also by the Ca^{2+} ions strongly interacting with carboxyl and hydroxyl groups localized in the pyranosic rings of these blocks. Although calcium ion helps to hold the blocks together, their polymeric nature bind the ion more firmly; this has been termed cooperative binding.

The investigations of Sikorski et al.[34] proved, that connected in such a way pairs of blocks belonging to several adjacent macromolecules, form the aggregates of pseudo-hexagonal order, with the average

Figure 8 Scheme of the "egg-box" zone (according to[33]) formed between the G blocks localized in two adjacent macromolecules. Black dots stand for the calcium ions.

TABLE V
Degree of Crystallinity of Investigated Fibers

Sample symbol	Degree of crystallinity [%]	Sample symbol	Degree of crystallinity [%]
AC1	27 ± 0.81	AH1	26 ± 0.78
AC2	31 ± 0.93	AH2	25 ± 0.75
AC3	31 ± 0.93	AH3	26 ± 0.78
AC4	30 ± 0.90	AH4	28 ± 0.84
AC5	32 ± 0.96	AH5	29 ± 0.87

distance between the axes of the neighboring macromolecules of a = 0.66 nm. Such a lattice constant results in the distance of d_{100} = 0.57 nm between the (100) lattice planes. In the diffraction curves of investigated samples, recorded with the wavelength of λ = 0.154 nm, the crystalline peak related to these planes is localized at $2\theta = 15.5^{o}$.

Sikorski et al.[34] have pointed out to the influence of calcium ions on the presence of crystalline reflections from (00*l*) lattice planes. As it is well known, in the case of macromolecules with a helical 2_1 conformation, the meridional reflexes with an odd value of *l* index are systematically absent.[34] This is the case of a "pure" polyguluronic acid. However, in the case of calcium alginate, the presence of strongly scattering Ca^{2+} ions, embodied between the adjacent G blocks causes, that the 2_1 symmetry is broken.[34] As a result, a crystalline reflection from (001) planes appears in the diffraction curve. In the WAXS curves of investigated fibers this peak is localized at $2\theta = 10.2^{o}$.

Calculated crystallinities of alginate fibers with the nanoadditive HAp and without it, as well as the sizes of crystallites existing in the fibers, are given in Tables V–VII.

The sizes of crystallites were determined from the width at half height of three strongest peaks in the diffraction curves of the fibers, using the Scherrer's

TABLE VI
Size of Crystallites in the Alginate Fibers Without the Nanoadditive

Sample symbol	D_{100} (M) [nm]	$D_{110/011}$ (G) [nm]	D_{101} (M/G) [nm]
AC1	5.5	5.0	5.4
AC2	4.6	4.5	5.3
AC3	5.8	5.7	5.4
AC4	5.3	5.2	5.3
AC5	5.7	5.3	5.1

D_{100} (M) – average size of crystallites in the direction perpendicular to the planes (100) in crystallites formed of M blocks.

$D_{110/011}$ (G) – average size of crystallites in the direction perpendicular to the planes (110) and (011) in crystallites formed of G blocks.

D_{101} (M/G) – average size of crystallites in the direction perpendicular to the planes (101) both in crystallites formed of M and G blocks.

TABLE VII
Size of Crystallites in the Alginate Fibers Containing the Nanoadditive HAp

Sample symbol	D_{100} (M) [nm]	$D_{110/011}$ (G) [nm]	D_{101} (M/G) [nm]
AH1	4.3	6.3	6.2
AH2	5.3	5.3	5.3
AH3	5.5	5.3	6.1
AH4	4.3	4.6	4.8
AH5	4.5	4.8	5.4

The symbols used are explained in the legend of Table VI.

formula (Fig. 5). The first peak corresponds to the family of planes (100) in the crystallites formed of mannuronic blocks. The second is composed of two overlapping reflections which correspond to the planes (110) and (011) in the crystallites composed of guluronic blocks. The third one results from the superposition of two very close reflections, related to (101) planes both in G and M crystallites. The values collected in Tables VI and VII represent the average sizes of crystallites in the directions perpendicular to the respective planes.

Comparing the data given in Tables IV and V one can notice, that the degree of crystallinity slightly increases with an increase in the as spun draw ratio. However, no correlation between the degree of crystallinity and the total draw ratio can be stated. Such a regularity is observed both for the fibers with the nanoadditive and without it. This fact indicates that the formation of the crystalline structure occurs solely during the solidification of the fiber material, before the drawing stage. An increase in the as spun draw ratio helps in a better orientation of macromolecules along the fiber axis and their parallel, ordered arrangement. Thereby it creates better crystallization conditions. However, an increase in the degree of crystallinity is small (about 4%–5% when the as spun draw ratio grows from 50% to 120%) and generally the crystallinity level in the investigated samples is low. Most probably, this is caused by a high concentration of calcium ions in the fibers material. A negative influence of the Ca^{2+} ions has already been reported in the literature,[34,35] but so far no explanation has been proposed.

Analyzing the literature data and the results obtained in this work, we come to the conclusion, that the lowered crystallization ability is connected with the formation of the "egg-box" zones, that arise between the pairs of G blocks located in two adjacent macromolecules of alginate.

As it has been proved in several articles,[33,34,36] only one pair of G blocks, located in two macromolecules of favorable orientation, is involved in the formation of the "egg-box" zone - Figure 9. So, the formation of bigger aggregates composed of such joined together pairs of G blocks, can occur only in the second stage – when thanks to some external factors or random events, many junction zones will be arranged in parallel to one another, creating a crystallite in this way. It is quite obvious, that the ordering and parallelization of the pairs of tangled macromolecules, connected with each other by short junction zones, is much more difficult than ordering of individual macromolecules. All the more, that the macromolecular chains are very stiff. Besides, the "egg-box" zones between G blocks, diminish the conformational freedom of the remaining parts of macromolecules, also those containing the mannuronic blocks and hinder their ordering. For these reasons, the number of arising crystallites and their sizes are much smaller than in the case of "pure" alginate acids. Moreover, the quality of the crystalline structure in the crystallites formed of the pairs of G blocks bonded by the "egg-box" zones is lower. As it has been shown by Sikorski et al.,[34] at least part of those crystallites is characterized by a quasi-hexagonal packing of chains so, they represent much lower degree of ordering than the crystalline structure of "pure" polyguluronic acid.

Further drawing of the alginate fibers after solidification, should undoubtedly improve to some degree the orientation of macromolecular chains in the amorphous regions, but does not contribute to an increase in the degree of crystallinity. It seems that the main factors which makes such an increase impossible are: (1) the alternating, block structure of the chains preventing from crystallization even in the case of parallel arrangement of the chains (the blocks of the same type should be adjacent to one another), (2) stiffening of the amorphous regions because of the presence of the "egg-box" zones.

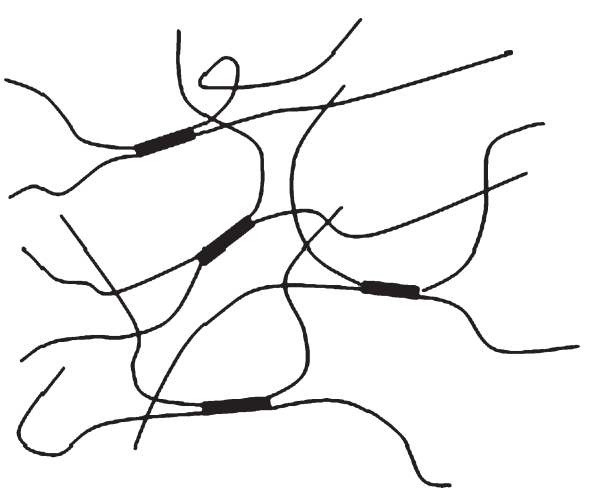

Figure 9 Schematic presentation of the gel structure formed during solidification of the alginate fibers. The thicker sectors stand for the "egg-box" zones between the adjacent macromolecules.

TABLE VIII
Strength Properties of Calcium Alginate Fibers with and Without Nanoadditive

Sample symbol	As-spun draw ratio [%]	Total drawing [%]	Total deformation	Drawing stress [cN/tex]			Tenacity [cN/tex]	Elongation at break [%]
				σ_0	σ_1	σ_2		
AC 1	50	101.78	3.0267	0.029	1.585	1.143	24.32 ± 0.66	8.83 ± 0.45
AC 2	70	120.40	3.7468	0.030	2.719	2.156	28.07 ± 0.68	10.00 ± 0.39
AC 3	90	109.18	3.9744	0.044	2.644	3.224	24.06 ± 0.81	8.62 ± 0.34
AC 4	110	87.81	3.9440	0.060	2.703	2.695	23.96 ± 0.97	8.38 ± 0.47
AC 5	120	97.00	4.3340	0.063	2.889	2.852	22.52 ± 0.90	7.71 ± 0.39
AH 1	50	110.66	3.1599	0.026	1.916	1.665	24.39 ± 1.37	9.27 ± 0.61
AH 2	70	103.58	3.4608	0.050	2.628	2.291	26.03 ± 0.97	9.77 ± 0.44
AH 3	90	97.90	3.7601	0.053	2.657	2.839	24.13 ± 0.86	9.41 ± 0.48
AH 4	110	99.72	4.1942	0.051	2.965	3.198	20.53 ± 0.94	7.79 ± 0.45
AH 5	120	76.92	3.8923	0.056	2.317	1.718	22.17 ± 0.73	9.65 ± 0.46

σ_0 – stress in the solidification process; σ_1 – stress in the first drawing process (plastification bath); σ_2 – stress in the second drawing process (saturated water vapour at a temperature of 135°C).

As it results from the Table V, the crystallinity of fibers with Hap is slightly lower: 2%–3%, than that one of fibers without the nanoadditive. However in both cases, the changes of crystallinity as a function of the as spun draw ratio, have the same character. Most probably, the presence of HAp grains in the solidifying stream is an additional impediment for the macromolecules to assume a configuration making the formation of crystallites of G and M type possible.

The sizes of crystallites determined from the widths of crystalline peaks related to different families of lattice planes lie in the range from 4.3 to 6.3 nm. So, they are very small which is favorable from the point of view of the fibers destination as the components of biocomposites.

No clear correlation between the size of crystallites and the forming conditions has been noticed. The differences between the sizes of guluronic and mannuronic crystallites are smaller than the limit of experimental error which is of the order of 1 nm, because of considerable overlapping of peaks (Fig. 7).

Analysis of the strength properties

Analysing the influence of the as-spun draw ratio and the total draw on the strength properties of the fibers leads to a conclusion that, both in the case of fibers with and without HAp nanoadditive, the greatest tenacity is displayed by fibers formed at the as-spun draw ratio of +70% (Table VIII, Figures 10 and 11). In the case of fibers without the

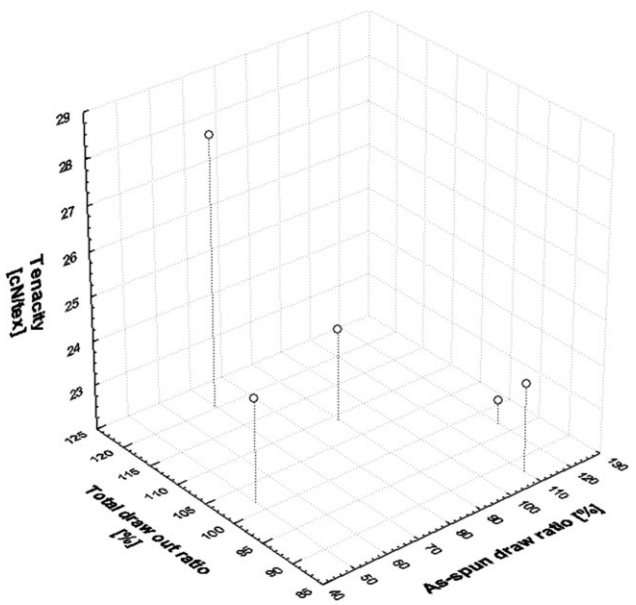

Figure 10 Tenacity as a function of the as-spun draw ratio and the total draw ratio for alginate fibers without the nanoadditive.

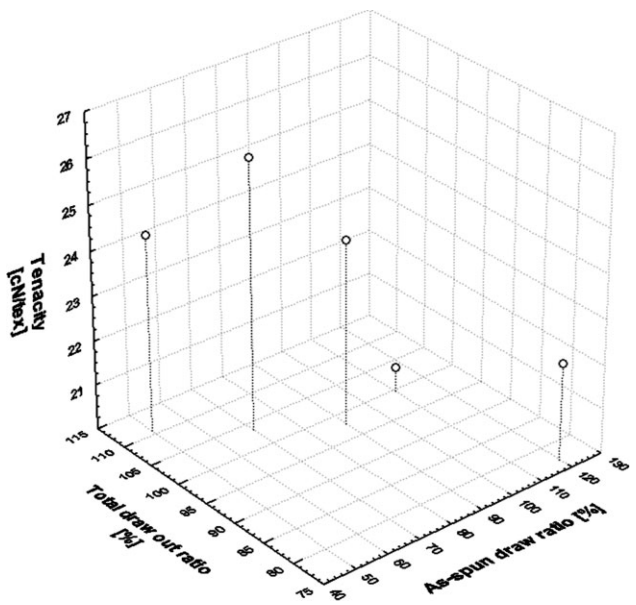

Figure 11 Tenacity as a function of the as-spun draw ratio and the total draw ratio for alginate fibers with the nanoadditive.

nanoadditive, this corresponds to the highest total drawing parameter in the series. For fibers containing HAp the drawing parameter is also one of the highest; however, it is lower than the one obtained in the case of the as-spun draw ratio of +50%. To account for this fact, it must be noted that for these fibers the formation of the structure at this stage took place under the influence of higher stress (Table VIII). This is because the final strength properties of the fibers depend not only on the degree of deformation at the drawing stage, but also on the value of stress due which the deformation processes are fulilled.

In the case of fibers without the nanoadditive, formed at the as-spun draw ratio of +50% and +70%, and at identical stress values at the solidification stage, the factor that determines higher tenacity values was the obtainable total draw ratio. In comparison to that, in fibers with the HAp nanoadditive, the formation of structure at the solidification stage took place under the influence of stress almost twice as strong, compared to the AH1 sample. Despite the lower susceptibility of the structure to deformation, this determined the highest specific tenacity in the series. As Table IV indicates, further raising of the as-spun draw ratio value entails the development of a structure that is less and less susceptible to deformation at the drawing stage (R_c value drops). Furthermore, the longitudinal rate gradient related to the use of increasingly higher filler extraction values goes up. Owing to this, structural elements are more ordered and "concentrated." Such a structure is less susceptible to deformation at the drawing stage, especially with a rigid structure of the macromolecule. Another difficulty is posed by the presence of the so-called "egg-box" bonds between the macromolecules. This explains the reduction of drawing parameters obtained as the as-spun draw ratio increases. At the same time, the stress value at the solidification stage varies slightly in the case of fibers containing the nanoadditive or tends to grow in the case of fibers without it. The characteristic feature is that, for both kinds of fibers formed with the application of the lowest value of the as-spun draw ratio, the drawing process occurs at stress values lower by 1-1.3 cN/tex than those present at the drawing of fibers formed at higher as-spun draw ratio. During the deformation processes, the fibers become further reinforced. This fact is proved by the tenacity growth by 2 cN/tex observed in the case of a sample formed at the as-spun draw ratio of +70%, after the second drawing stage in comparison to the tenacity value following the plastification drawing. High tenacity values displayed by fibers formed at the as-spun draw ratio of +70% are compliant with the nature of their porous structure. Both types of fibers with the highest tenacity value are characterised by a less macroporous structure. The maximum, with regard to very large pores, has decreased (Fig. 4). In the case of fibers without the nano-additive, the proportion of very small pores is the highest compared with other fibers. This is demonstrated in the pore size distribution curve by the distinct maximum in this range. Meanwhile, fibers containing the nanoadditive are distinguished by the occurrence of a broad maximum with regard to medium-sized pores. In both cases the combined proportion of small and medium-sized pores ranges between 30.77% and 55.32%. The influence of the nanoadditive in the material is distinct in the case of fibers formed at the as-spun draw ratio of +70%. Their tenacity value is lower by 2 cN/tex in comparison to fibers without the nanoadditive. This is caused mainly by the lower susceptibility of the structure formed at the solidification stage to deformation processes during drawing. Higher tensile stress values during solidification (with similar values at the subsequent process stages) may result from the increased internal friction of the system. This effect occurs mainly during solidification. However, no growth of the total pore volume was observed (as it was in the case with other fiber-forming materials), but only a deepening in the macroporous nature of the structure is observed. This is because fibers containing the nanoadditive are generally characterised by a smaller internal surface in comparison to fibers without the nanoadditive.

Analyzing all factors influencing the mechanical properties of investigated alginate nanocomposite fibers one have to emphasize, that they substantially depend on the number of the "egg-box" zones where the G blocks from two different macromolecules are bonded with one another not only by the hydrogen bonds but also thanks to the coordination of calcium ions localized in between them. These ions strongly interact with carboxyl and hydroxyl groups of the pyranosic ring belonging to adjacent G blocks. The number of such zones is dependent on the degree of substitution of the sodium ions by the calcium ions which in turn is determined by the average content of calcium in the fibers.

The results reported by Fabia et al.[35] prove that the content of calcium has a bigger influence on the tenacity of alginate fibers than their degree of crystallinity. Fabia et al.[35] have found, that when the calcium content rises, the tenacity of the fibers also increases, despite of a considerable drop in their crystallinity. Such a dependence can be fully explained when we adopt the analysis presented in paragraph 3.4. An increase in the Ca^{2+} ions content causes, that the number of the "egg-box" junctions between the macromolecules increases. The ordering and parallelization of these pairs of macromolecules, bonded with one another by such junctions is much

more difficult than in the case of individual macromolecules. As a result, the ability of the fiber material to crystallization decreases and the degree of crystallinity diminishes. However, the "egg-box" junctions between the macromolecules considerably strengthen the amorphous regions, and make all material more consistent and stiffer. Finally, despite of a decrease in the volume fraction of crystalline regions in the fibers, their specific tenacity rises.

In the investigated fibers, formed at the same composition of the coagulation bath, the degree of substitution of sodium ions by calcium ions is on a comparable level. Slightly higher calcium content in the fibers with HAp is caused by the presence of the nanoadditive containing this element, dispersed in the fiber material.

For both types of fibers, the changes in the elongation at break as a function of the as spun draw ratio, lie in the range 7.7%–10%.

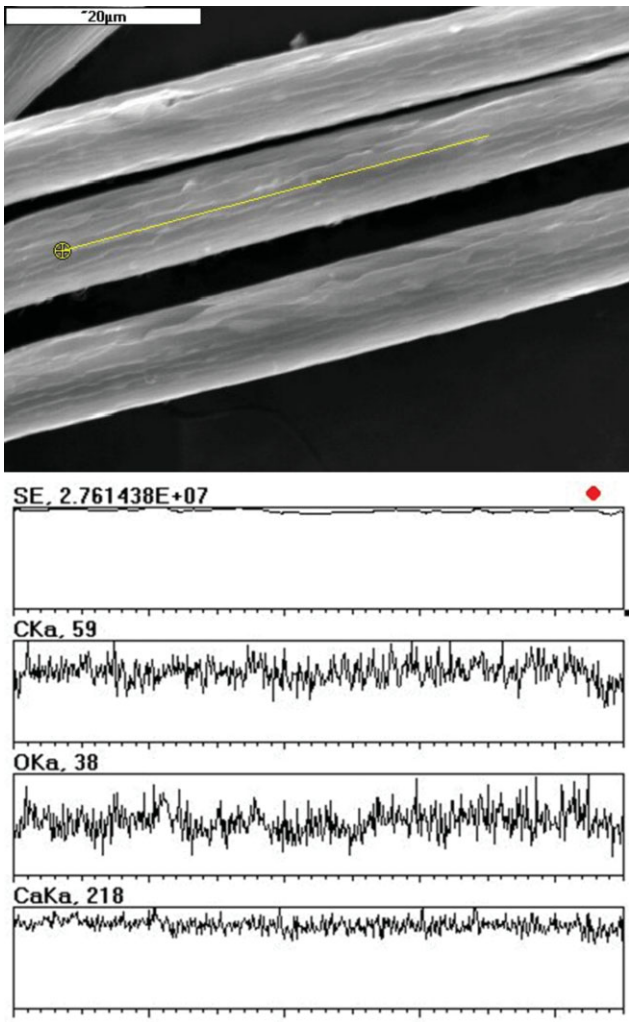

Figure 12 SEM + EDS linear analysis for fibers containing HAp nanoadditive. [Color figure can be viewed in the online issue, which is available at www.interscience.wiley.com.]

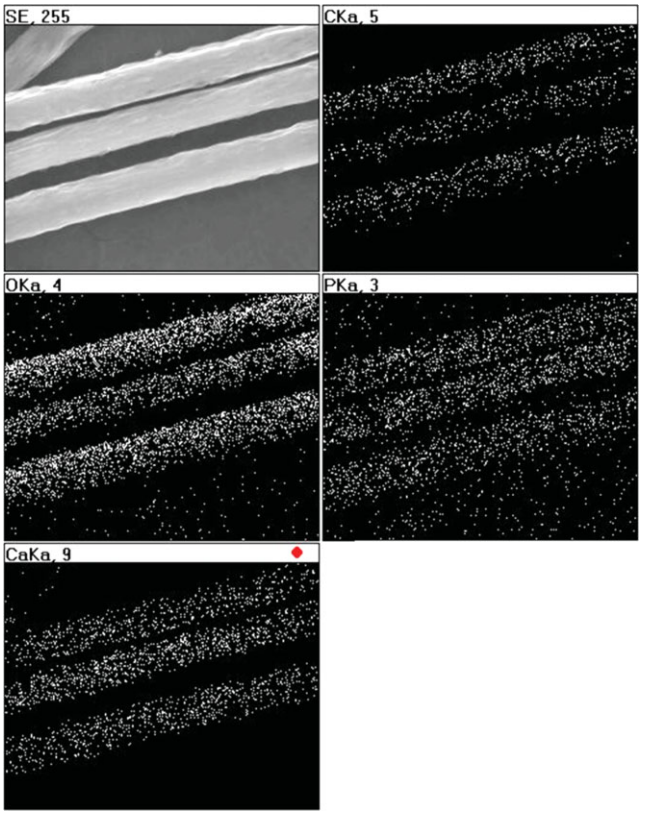

Figure 13 The map of elements characteristic of fibers containing HAp nanoadditive. [Color figure can be viewed in the online issue, which is available at www.interscience.wiley.com.]

SEM + EDS analysis

Our research included an SEM + EDS analysis to demonstrate the presence of hyroxyapatite on the surface of calcium alginate fibers into which this nanoadditive was introduced. Moreover, based on this analyses, we attempted to evaluate the uniformity of nanoadditive distribution on the fiber surface. The conducted linear analysis (Fig. 12) reveals that, on the fiber fragment under examination, this distribution is rather even. The map of characteristic elements in the examined area shown in Figure 13 presents the occurrence of areas of equal nanoadditive distribution, which is particularly evident on the phosphorus distribution map.

CONCLUSIONS

Strong sorptive properties of calcium alginate fibers, both with and without the HAp nanoadditive, are determined by the hydrophilic nature of the material. Despite the differences in fiber porosity, the effect of the filler extraction and presence of nanoadditive HAp in the fibers on the value of the indicators is minor. Both fiber types show similar moisture sorption at 65% RH at a level of 24.07%–25.40%

and minor differences in moisture sorption at 100% RH at a level of 44.5%–48.2%. Water retention values are related not only to the total pore volume, but mainly to the macroporous nature of the structure. Owing to the structure, there is a significant capability of binding, through hydrogen bridges, of polymorphic water clusters in very large pores (not larger than 5000 nm). The deepening of the macroporous nature of the structure is the reason for the occurrence of higher retention values in fibers containing HAp.

At comparable degrees of calcium-for-sodium ion substitution in the fiber material, their strength properties are mainly related to the structure formed at the solidification stage, the stress values during deformation, and the value of the total draw out ratio.

A stiff structure of alginate macromolecules and the presence of "egg-box" zones between the chains of macromolecules causes, that the tenacity of the fibers are considerably influenced by the deformation of a still liquid stream of fiber material. The deformation depends directly on the as-spun draw ratio.

A large number of the junction zones of the "egg-box" type, caused by a high content of the calcium ions is the main reason of a relatively low crystallinity of the fibers, resulting simultaneously in their good tenacity.

The presence of the HAp nanoadditive in the material of alginate fibers formed at the as-spun draw ratio of +70% decreases their susceptibility to deformation in the drawing stage, and results in their tenacity being lower by 2 cN/tex than of the fibers with no nanoadditive.

Because of the possibility of obtaining a tenacity value exceeding 26 cN/tex, accompanied by high sorptive and water retention properties of 90%, it is advantageous to form nanocomposite alginate fibers containing HAp at the as-spun draw ratio of +70%.

The level of these properties, as well as the presence of HAp nanoadditive in the material, predisposes it for being applied as a component of biocomposites supporting the process of bone tissue regeneration.

References

1. Kong, H. J.; Kaigler, D.; Kim, K.; Mooney, D. J. Biomacromolecules 2004, 5, 1720.
2. Draget, K. I.; SkjK-Bræk, G.; Simdsrød, O. Int J Biol Macromol 1997, 21, 47.
3. Mørch, Y. A.; Donati, I.; Strand, B. L.; Skjåk-Bræk, G. Biomacromolecules 2007, 8, 2809.
4. Hashimoto, T.; Suzuki, Y.; Yamamoto, E.; Tanihara, M.; Kakimaru, Y.; Suzuki, K. Biomaterials 2004, 25, 1407.
5. Bouhadir, K. H.; Lee, K. Y.; Alsberg, E.; Damm, K. L.; Anderson, K. W.; Mooney, D. J. Biotechnol Prog 2001, 17, 945.
6. Alsberg, E.; Anderson, K. W.; Albeiruti, A.; Franceschi, R. T.; Mooney, D. J. J Dent Res 2001, 80, 2025.
7. Chung, T. W.; Yang, J.; Akaike, T.; Cho, K. Y.; Nah, J. W.; Kim, S. I.; Cho, C. S. Biomaterials 2002, 23, 2827.
8. Nie, H.; He, A.; Zheng, J.; Xu, S.; Li, J.; Han, C.hC. Biomacromolecules 2008, 9, 1362.
9. Despang, F.; Bernhardt, A.; Hanke, T.h; Pompe, W.; Gelinsky, M. J Am Ceram Soc 2007, 90, 1703.
10. Sakai, S.; Yamaguchi, S.; Takei, T.; Kawakami, K. Biomacromolecules 2008, 9, 2036.
11. Błażewicz, S.; Stoch, L. Biomateriały Tom 4"; Akademicka Oficyna Wydawnicza Exit: Warszawa, 2003.
12. Katti, K. S. Colloid Surf B 2004, 39, 133.
13. Van Blitterswijk, C. A.; Grote, J. J.; Kuijpers, W.; Daems, W. T.; De Groot, K. A. Biomaterials 1986, 7, 553.
14. Chen, Q. Z.; Wong, C. T.; Lu, W. W.; Cheung, K. M. C.; Leong, J. C. Y.; Luk, K. D. K. Biomaterials 2004, 25, 4243.
15. Le Geros, R. Z. Clin Mater 1993, 14, 65.
16. Weiner, S.; Wagner, H. D. Annu Rev Mater Sci 1998, 28, 271.
17. Loupasis, G.; Hyde, I. D.; Morris, E. W. Arch Orthop Traum Su 1998, 117, 132.
18. De Groot, K. Ceram Int 1993, 19, 93.
19. Chen, F.; Wang, Z. C.; Lin, C. J. Mater Lett 2002, 57, 858.
20. Deng, X.; Hao, J.; Wang, C. Biomaterials 2001, 22, 2867.
21. Haberko, K.Polish Patent No. P-359960, 2003.
22. Rabiej, M.; Rabiej, S.Analiza rentgenowskich krzywych dyfrakcyjnych polimerów za pomocą programu komputerowego; WAXFIT Publishing House ATH: Bielsko-Biała, 2006.
23. Rabiej, M. fibers Text Estern Eur 2003, 11, 83.
24. Rabiej, M. Polimery 2003, 48, 288.
25. Ferguson, J.; Kembłowski, Z. "Reologia stosowana płynów"; Wydawnictwo Marcus sc: Łódź, 1995.
26. Mikołajczyk, T.; Boguń, M. Fibres Text East Eur 2005, 13, 28.
27. Wołowska-Czapnik, D. "New Generation Alginate Fibers from Medical Application", Doctoral Thesis, Technical University of Lodz, 2006.
28. Mikołajczyk, T.; Rabiej, S.; Boguń, M. J Appl Polym Sci 2006, 101, 760.
29. Lipp-Symonowicz, B. "Physico-chemical aspekt of fibre dyeing and optical brightening"; Polish Academy of Science: Łodz, 2003.
30. Atkins, E.; Nieduszynski, I.; Mackie, W.; Parker, K.; Smolko, E. Biopolymers 1973, 12, 1865.
31. Draget, K. I.; Smidsrod, O.; Skjak-Braek, G. "Alginates from Algae", "Polysacharides and Polyamides in the Food Industry, Properties, Production and Patents", Steinbuchel, A.; Rhee, S. K., Eds. WILEY-VCH Verlag Gmbh & Co. KGaA: Weinheim, 2005.
32. Grant, G.; Morris, E.; Rees, D. A.; Smith, P. J. C.; Thom, D. FEEBS Lett 1973, 32, 195.
33. Smidsr D, O. J Chem Soc Faraday Trans 1974, 57, 263.
34. Sikorski, P.; Frode, M.; Skjak-Bræk, G.; Stokke, B. T. Biomacromolecules 2007, 8, 2098.
35. Fabia, J.; Ślusarczyk, C.; Gawłowski, A.; Graczyk, T.; Włochowicz, A.; Janicki, J. Fibres Text Estern Eur 2005, 13, 114.
36. Morris, E.; Rees, D. A.; Thom, D.; Boyd, J. Carbohydr Res 1978, 6632, 14595.